

Exploring novel high power density concepts for attractive fusion systems

Mohamed A. Abdou *, The APEX Team

Mechanical and Aerospace Engineering Department, University of California Los Angeles, 44-114 Engineering IV, Los Angeles, CA 90095, USA

Received 5 October 1998; received in revised form 15 January 1999

Abstract

The Advanced Power Extraction (APEX) study is aimed at exploring innovative concepts for fusion power technology (FPT) that can tremendously enhance the potential of fusion as an attractive and competitive energy source. Specifically, the study is exploring new and ‘revolutionary’ concepts that can provide the capability to efficiently extract heat from systems with high neutron and surface heat loads while satisfying all the FPT functional requirements and maximizing reliability, maintainability, safety, and environmental attractiveness. The primary criteria for measuring performance of the new concepts are: (1) high power density capability with a peak neutron wall load (NWL) of $\sim 10 \text{ MW m}^{-2}$ and surface heat flux of $\sim 2 \text{ MW m}^{-2}$; (2) high power conversion efficiency, $\sim 40\%$ net; and (3) clear potential to achieve high availability; specifically low failure rate, large design margin, and short downtime for maintenance. A requirement that $\text{MTBF} > 43 \text{ MTTR}$ was derived as a necessary condition to achieve the required first wall/blanket availability, where MTBF is the mean time between failures and MTTR is the mean time to recover. Highlights of innovative and promising new concepts that may satisfy these criteria are provided. © 1999 Elsevier Science S.A. All rights reserved.

Keywords: Fusion; Reactor; Wall load limits; Blanket; First wall

1. Introduction

The most important task for fusion energy research over the next two decades is to develop a vision for an attractive product. The attributes of an attractive product are economics, safety, and environmental impact. World-wide fusion system

studies have shown that a fusion energy system can be designed to have important safety and environmental advantages compared to other energy sources [1,2].

However, developing a vision for an economically competitive fusion system remains the grand challenge for fusion researchers. Meeting this challenge requires advances in plasma physics and in fusion technology. A key element in technology is Fusion Power Technology (FPT). FPT is concerned with all components in the immediate exte-

* Corresponding author. Tel.: +1-310-2060501; fax: +1-310-8252599.

E-mail address: abdou@fusion.ucla.edu (M.A. Abdou)

rior of the plasma, commonly called ‘in-vessel system’, which include first wall, divertor, blanket, and the vacuum boundary. The functional requirements of FPT are given in Table 1. FPT has many engineering science and technology development issues whose resolution, together with the development of simple plasma confinement configurations, will be the most important element in determining the economic competitiveness of fusion energy systems. This will be analyzed in Section 2. Limitations of current concepts will be derived and analyzed.

The APEX study was initiated as part of the U.S. Fusion Energy Sciences program initiative to identify a vision for an attractive fusion energy system. The purpose of the study is to explore and identify novel, possibly revolutionary concepts for in-vessel components that can substantially enhance the economic competitiveness of fusion energy systems. A special emphasis is achieving high power density capability. The specific objectives of APEX will be summarized in Section 3.

APEX provides a research environment conducive to innovation. The study covers conceptual design, modelling, and experiments for new and revolutionary ideas. Some of the new ideas and the early results from design conceptualization and analysis will be presented in Section 4.

2. Key technology issues impacting economics

Understanding the major influence of FPT on economics and identifying the most critical FPT issues can be facilitated by examining a simplified formula for the ‘bus-bar’ cost of energy (COE):

$$\text{COE} \sim \frac{C \cdot i + R + O}{P \cdot A \cdot M \cdot \eta} \quad (1)$$

where C is the capital cost, i is a fixed charge rate, R is the annual replacement cost, O is the annual operation and maintenance cost, P is the fusion power, A is plant availability, M is energy multiplication in the in-vessel components, and η is the net thermodynamic efficiency. (Background

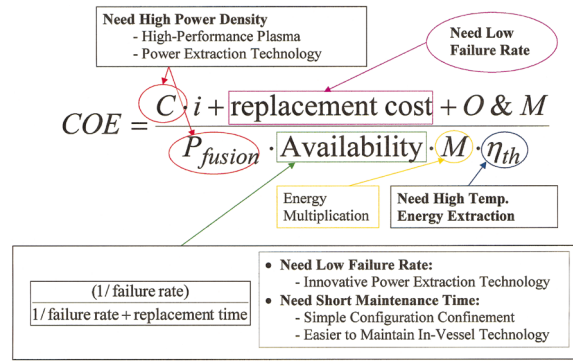


Fig. 1. Fusion power technology is critical to fusion energy.

information on economics of fusion systems can be found in the literature; see [3–5]).

The role of FPT in-vessel components in achieving lower cost of energy can be inferred from examining the key factors in Fig. 1 as discussed above.

2.1. Power density

A lower COE requires a higher P/C ratio. For a given unit cost of materials, this means higher power density (HPD). The two most important requirements for obtaining practical HPD systems are: (a) high power production per unit volume of the plasma; and (b) FPT in-vessel components that can handle the high surface heat flux and high neutron wall load (NWL) on the first wall in such HPD systems.

Two questions will now be addressed. The first concerns the goal for the wall load and the second relates to the limits on wall loads in current first wall/blanket systems.

Table 1

Functional requirements of fusion power technology

Provision of VACUUM environment
EXHAUST of plasma burn products
POWER EXTRACTION from plasma particles and radiation (surface heat loads)
POWER EXTRACTION from energy deposition of neutrons and secondary gamma rays
TRITIUM BREEDING at the rate required to satisfy tritium self sufficiency
RADIATION PROTECTION

2.1.1. Goals for wall load

Fission reactors represent a class of energy system with which fusion must compete. Table 2 shows the average core power density in MW m^{-3} in several types of fission reactors: Pressurized Water Reactor (PWR), Boiling Water Reactor (BWR), High-Temperature Gas-Cooled Reactor (HTGR), and Liquid-Metal Fast Breeder Reactor (LMFBR). Shown for comparison is the average core power density for a fusion power reactor based on the ‘ITER-type’ traditional tokamak. We assume the NWL to be 3 MW m^{-2} , i.e. a factor of 3 higher than the 1 MW m^{-2} wall load in ITER, while we hold the volume the same. In other words, we assume a factor of 3 improvement in power density beyond ITER, which is justified based on tokamak reactor studies. In calculating the average core power density for the fusion system we use only the volume of materials in the ‘in-vessel’ components and the magnets. We exclude the volume of void regions such as the plasma.

Table 2 shows that the average core power density in a fission reactor is higher than in an ITER-type reactor by a factor, f , of ~ 80 , 7.5, and 200 for PWR, HTGR, and LMFBR, respectively. If fusion reactors are to achieve the same average power density, the NWL will need to be in the range 22–600 MW m^{-2} . Such high wall loads may be impossible to achieve and handle in current magnetic fusion concepts.

A detailed economic analysis is beyond the scope of this paper. However, some simple arguments are enlightening. The cost of a power plant

consists mainly of the cost of the reactor core plus the cost of the balance of plant (BOP). Reactor studies indicate that the cost of the BOP in fission and fusion are comparable. The BOP cost tends to be in many cases roughly half the total cost in a fission power plant. If the fusion core is twice as expensive as that of a fission core, the capital cost of a fusion plant will only be $\sim 50\%$ higher than that of fission. Assuming that the plant availability is the same in fission and fusion, the COE for fusion would be $\sim 50\%$ higher than fission.

Fusion has clear safety and environmental advantages over fission. Therefore, fusion can be expected to be acceptable at a somewhat higher cost than fission. Exactly how much higher COE society is willing to accept is difficult to predict. However, an increment in COE of more than 50% does not seem likely to be acceptable.

From the above analysis, it is clear that fusion research should set a goal for the NWL to be greater than 10 MW m^{-2} in order to enhance the potential of economic competitiveness for fusion systems. At 10 MW m^{-2} , the average power density will be about half of that in HTGR, which has the lowest power density of fission reactor systems.

In Table 2, the peak to average heat flux at the coolant interface is shown. This ratio is ~ 2.8 for PWR, 12.8 for HTGR, 1.43 for LMFBR and 50 for an ITER-type fusion system. The high peak to average heat flux ratio in fusion systems implies that the technological difficulty of the energy extraction system is comparable to that in fission reactors, despite the lower average power density

Table 2
Power density and heat flux in fission reactors compared to fusion with traditional evolutionary concepts

	PWR	BWR	HTGR	LMFBR	Fusion ^a at 3 MW m^{-2}
Equivalent core diameter (m)	3.6	4.6	8.4	2.1	30
Core length (m)	3.8	3.8	6.3	0.9	15
Average core power density (MW m^{-3})	96	56	9	240	1.2 ^b
Peak-to-average heat flux at coolant interface	2.8	2.6	12.8	1.43	50 ^c

^a Based on a tokamak power reactor of the ‘ITER-type’, where the fusion power is scaled up from ITER by a factor of 3, corresponding to a neutron wall load of 3 MW m^{-2} , while keeping the reactor volume the same.

^b Average core power density is obtained using only the volume of materials in the in-vessel components and the magnets. The volume of ‘void’ regions such as the plasma is excluded.

^c Peak is at the divertor.

Table 3

Current world-wide concepts for first wall/blanket (all concepts use a solid structural material for first wall)

Breeder*	Coolant	Structural material
Solid Breeder (Li ₂ O, Li ₄ SiO ₄ , Li ₂ ZrO ₃ , Li ₃ TiO ₃)	He or H ₂ O	Ferritic steel, SiC composites
Self-cooled liquid metal breeder (Li, LiPb)	Li, LiPb	Ferritic steel and V _{alloy} (with electric insulator), SiC composite with LiPb only
Separately-cooled liquid-metal breeder		
Li	He	Ferritic steel, V _{alloy}
LiPb	He or H ₂ O	Ferritic steel, V _{alloy} , SiC composites

* Some designs in Japanese Universities consider the molten salt flibe as breeder/coolant.

in fusion. Enhancing the potential competitiveness of fusion, while keeping the technological difficulty manageable, requires incorporating physics and technological schemes to reduce the peak to average ratio.

2.1.2. Wall load limits of current concepts

In this section, we derive the limits on the NWL capability of first wall/blanket concepts that are currently being pursued world-wide. The last 25 years of world-wide research identified the concepts in Table 3, which are now the focus of R&D in the major world fusion programs. All concepts use ‘bare’ first wall, i.e. solid structural material in the first wall directly exposed to the plasma. These concepts are documented in the literature [6–12].

Calculations were performed to determine the NWL limits for ‘bare’ solid first wall. The first wall structural materials evaluated included two groups. The first group included the so-called ‘low-activation’ materials, i.e. Ferritic Steel, V–Cr–Ti alloys, and SiC–SiC composites. The second group included high-temperature refractory alloys, alloys of Niobium (Nb–1Zr), Tantalum (T111), Molybdenum (TZM), and Tungsten, which offered the potential for high performance but do not satisfy the ‘low activation’ criterion. In addition, Oxide-Dispersed Steel (ODS) has also been evaluated.

Table 4 shows the key material properties used in the calculations averaged over a relevant temperature range. The maximum practical operating temperature limit is also shown in Table 4. For an explanation of the database, see Refs. [13–18].

- The solid first wall is modeled as a 5 mm thick plate cooled from one side, subjected to plasma radiation on the other side as well as nuclear bulk heating, and is allowed to expand but not bend. Only for the SiC–SiC composite solid wall is the thickness considered to be 4 mm. It should be noted that the actual stresses may be higher if the first wall is restrained by a second wall or blanket. They may be lower if the wall is allowed to bend.
- The radiation heat flux is taken to be 0.2 MW m⁻² per 1 MW m⁻² NWL. This means that 80% of the alpha power is radiated to the first wall. Since the first wall has typically more than ten times the area of the divertor, radiating most of the alpha power seems logical. The nuclear heating in the FW is assumed to be 10 W cm⁻³ per 1 MW m⁻² NWL.
- No peaking factors are considered. If a peaking factor is to be considered, the NWL limits shown should be scaled by the peaking factor to determine the average NWL.
- Stress limits for the metallic alloys are taken to be functions of the average wall temperature and no radiation effects are considered. Temperature-averaged values of other material properties are used in the calculations.
- The wall temperature profile is parabolic due to the combined bulk and surface heating. The thermal stress, however, is considered to be proportional to the temperature drop across the wall.
- A primary stress of 20 MPa was considered, corresponding to hoop stress due to coolant pressure and other constraints. This is an ap-

proximation and the actual value of that stress may be different.

- For the metallic alloys, the stress-limited NWL limits were determined by comparing the total (thermal plus primary) stress to $3S_m$, where $S_m = \min \sigma_{UTS}/3, 2\sigma_Y/3$. In the case of SiC–SiC composites, the NWL limit was calculated by direct comparison of the induced stress to the material stress limit (either matrix cracking stress or the ultimate tensile stress) guidelines for the structural limits of metallic alloys can be found in [19].

The stress criterion used here to find the NWL limits for metallic alloys is a conventional criterion which is used by the ‘Fusion Community’ to screen out and compare materials. For SiC–SiC composites, the situation is different. In order for the calculations to make sense, one should recall how the induced stresses cause the material to fail. For example, the simple addition of thermal stresses and primary stresses may not make sense, as these stresses lead to different failure paths/mechanisms. Primary stresses result from direct loading. These stresses are of the same nature as those applied during machine testing of materials samples. Therefore, if the induced stresses are mainly due to direct loading, (i.e. primary), it may be permissible to compare these stresses with one of the measured material failure stresses, even though this requires accounting for the material anisotropy in both deformation and failure, should we speak of SiC–SiC composites. However, if the induced stress is mainly due to temper-

ature gradients and/or constraining the structure while changing its temperature (even uniformly) the induced stresses lead to failure by mechanisms which are fundamentally different from those resulting during direct loading. In the simplest case of uniform changes in temperature of a (simple) structure made of composites with no constraints, microscopic stresses of large magnitude still develop due to the heterogeneous nature of the material. Even though these stresses average to zero at the macroscopic level, they can still result in severe damage of the material. Relevant details on the evolution of internal stresses in SiC–SiC composites under high-temperature neutron irradiation can be found in [20]. In violation of the argument just presented, the induced thermal stresses are compared with the matrix cracking stress or the ultimate stress limits for SiC–SiC composites, and the results should be looked at with these facts in mind.

Figs. 2 and 3 show the temperature-limited and the stress-limited NWL, respectively. These limits are defined as the values of the NWL at which the maximum operating temperature or design stress of the material is exceeded. The maximum operating temperatures for the materials: 700°C for V–Cr–Ti, 550°C for Ferritic steel, 700°C for ODS, 1000°C for SiC–SiC composites, 1300°C for T-111, 1100°C for Nb1Zr, 1200°C for TZM, and 1500°C for tungsten.

The assumptions used to assess the NWL limits for conventional FWs made out of the materials mentioned here are as follows:

Table 4

Properties of reference low activation and high-temperature refractory materials (properties are averaged over the temperature range relevant to calculations of the neutral wall load limit in this work)

Material	$T_{\max}(\text{°C})^*$	E (GPa)	ν	k (w m°C ⁻¹)	$\alpha(10^{-6} \text{ °C}^{-1})$	Temperature range (°C)
Ferritic steel	550	185	0.29	33	11.8	350–550
V–Cr–Ti	700	122	0.36	35	11.3	400–700
SiC–SiC	1000	270	0.2	10	2.75	RT–1000
ODS	700	(Approximated by ferritic steel)				
Nb1Zr	1100	104	0.39	55	9	500–1200
Tungsten	1500	360	0.29	115	4.5	500–1500
TZM	1200	222	0.32	100	5.8	400–1200
T111	1300	160	0.37	50	6.3	400–1300

* Based on thermal creep consideration for all metals; minimum saturation swelling for SiC–SiC.

NWL-BW-Temp

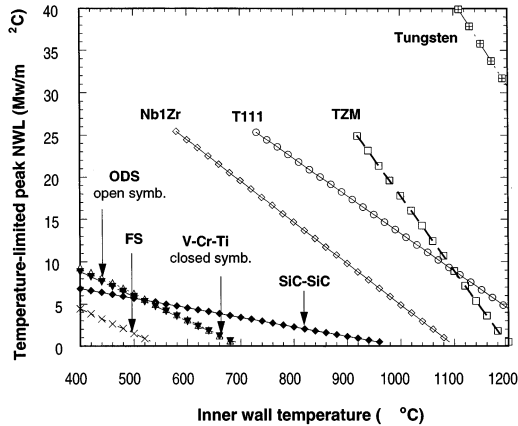


Fig. 2. Peak neutron wall load limits (NWL) for structural 'dry' first wall based on maximum temperature limits. The NWL shown is a function of the inner wall temperature, i.e. the interface temperature between the wall and the coolant.

The peak NWL limits are shown in Figs. 2 and 3 as a function of the inner wall temperatures, which is the minimum temperature in the structure, i.e. the interface temperature between the wall and the coolant. This interface temperature is equal to the sum of the average coolant temperature and the film temperature drop. The latter can

NWL-BW-Stress

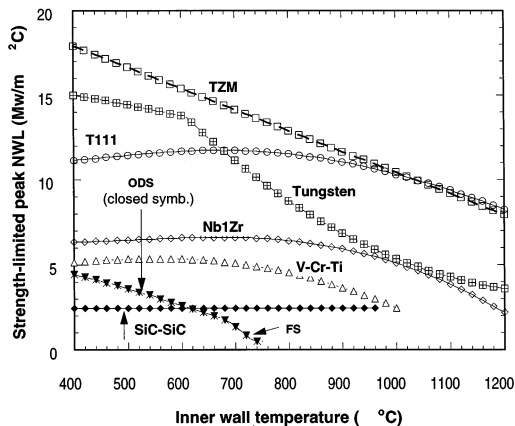


Fig. 3. Peak neutron wall load limits (NWL) for structural 'dry' first wall based on limits imposed by allowable stress criteria. The NWL is shown as a function of the inner wall temperature, i.e. the interface between the wall and the coolant.

vary typically from 50 to 300°C depending on the particular coolant, the coolant conditions, and the heat flux.

A key requirement for economic competitiveness is to attain a high coolant temperature. Exit coolant temperatures $> 600^{\circ}\text{C}$ are highly desirable in order to obtain a thermal conversion efficiency of $\sim 40\%$ or greater. This means that a wall coolant interface temperature (inner wall temperature) of $> 750^{\circ}\text{C}$ is highly desirable, which is higher than the capability of all 'low activation' materials. It is possible, however, that the coolant from the first wall is passed through the blanket to gain some additional heat. This allows reduction in the required interface temperature.

Figs. 2 and 3 show that the NWL drops rather rapidly with the interface temperature. Table 5 shows the peak NWL limits, both temperature-limited and stress-limited, for all materials considered here and for a coolant-wall interface temperature consistent with the temperature capability for each material. When comparing various materials it is important to note that lower thermal efficiencies will be obtainable with materials that have lower temperature capability. It should be noted that these results are based on a 5-mm thick first wall as mentioned previously. The allowable wall load will be higher for thinner walls and lower for thicker walls.

Important conclusions can be reached from examining Table 5. Ferritic steel is limited to a very low NWL of 1.5 MW m^{-2} if the interface temperature is 500°C . If the interface temperature is allowed to drop to 450°C , which will cause further reduction in thermal efficiency, the NWL increases to 2.9 MW m^{-2} . V alloys offer higher wall load capability: 3.2 and 4.7 MW m^{-2} for interface temperatures of 600 and 550°C , respectively. SiC/SiC composites are limited to a NWL of 2.5 MW m^{-2} . It should be noted here that although SiC/SiC composites are often described as innovative materials they are limited to poor performance, i.e. low NWL capabilities.

The high-temperature refractory alloys have much higher wall load capability than 'low-activation' materials. Nb-1Zr, W, TZM, and T111 have wall load limits of $\sim 6.6, 8.8, 13,$ and 11.6 MW m^{-2} , respectively.

Table 5
Peak neutron wall load limits for ‘dry’ first wall (for 5-mm thick wall)

Material	Maximum temperature (°C)	Wall-coolant interface temperature (°C)	Peak neutron wall load limit (MW m ⁻²)		
			Limited by maximum temperature	Limited by stress criterion	Maximum wall load
Ferritic steel	550	500	1.5	3.6	1.5
Ferritic steel	550	450	2.9	4	2.9
V–Cr–Ti	700	600	3.2	5.4	3.2
V–Cr–Ti	700	550	4.7	5.4	4.7
SiC–SiC	1000	700	3.5	2.5	2.5
ODS	700	600	3	2.6	2.6
Nb–1Zr	1100	600	24.5	6.6	6.6
Tungsten	1500	600	>30	8.8	8.8
TZM	1200	600	>25	13	13
T111	1300	600	22.3	11.6	11.6

Two very important conclusions can be derived from the above results. First, ‘dry’ solid first walls are severely limited in their capability to handle high power density (compare, for example, the power density obtained with these wall load limits to those obtained in fission reactors, see Table 2). Second, the class of material called ‘low activation’ materials imposes a heavy penalty on the economics of the fusion system because of the low wall load limits. The high temperature refractory alloys offer much HPD capability (but with an increased level of long-term radioactivity). It is possible that these high temperature refractory alloys can be used in the high power density region (first wall), while other lower activation materials are used in the rest of the blanket.

2.2. Availability, failure rate, maintenance

As shown in Fig. 1, the cost of energy is inversely proportional to the plant availability. The ‘in-vessel’ system will play a major role in the plant availability, A , as shown below.

Typical A for current commercial power plants is >75%, with a BOP availability of ~85%. Since the BOP in a fusion system is similar to that of current power plants, it is reasonable to assume the same BOP availability. Thus, a fusion reactor must achieve an availability of >(75/85), i.e. >88%. While improvements in BOP availability

may be possible in the future, such improvements are likely to be for both non-fusion and fusion power plants. Therefore, the reactor availability requirement of >88% is not likely to change.

A fusion reactor, such as the tokamak, has many components. These include: (1) toroidal magnets; (2) poloidal magnets; (3) plasma heating system (e.g. neutral beams and/or rf waves); (4) current drive system; (5) first wall/blanket system; (6) vacuum vessel; (7) bulk and penetration shields; (8) fueling; (9) tritium system; (10) impurity control and vacuum pumping. Reactor studies show that replacement of toroidal-field (TF) coils or some of the poloidal-field (PF) coils trapped below or inside the TF coils can take a very long time, much longer than a year. This places a burden on the availability requirement for the other reactor components. For simplicity, we assume here that the reactor has six major components with equal outage risk with the first wall/blanket (FW/B) being such a component. In this case, the required availability, A_{wb} , of first wall/blanket is >97.8%.

The availability of the first wall/blanket consists of two parts related to: (1) outage for scheduled maintenance; for example, to replace the first wall at the end of its ‘expected’ lifetime; and (2) outage due to unscheduled failures.

Let us first consider the case of scheduled outage to replace the first wall at the end of its

lifetime. If such a replacement is performed by simultaneously replacing all first wall/blanket sectors in 3 months, the first wall lifetime will need to be > 11 years in order for A_{wb} not to fall below 97.8%. This is a very demanding requirement on the first wall lifetime given the harsh radiation environment in the fusion system. One clever approach is to schedule the replacement of the first wall/blanket sectors to coincide with the plant outage for maintenance of the power plant. For example, if the plant is shutdown one month each year for routine maintenance, then approximately one-third of the FW/B sectors could be replaced annually. Therefore, a first wall lifetime of ~ 3 years may be adequate to avoid ‘availability penalty’ due to scheduled replacement of the FW/B.

The outage due to unscheduled failures is a much more complex and demanding issue, as we will show next. The outage due to failure has substantial effect on availability as experience from current power plants show [22]. ‘Failure’ is different from design lifetime. ‘Failure’ is defined [21–23] as the ending of the ability of a design element to meet its function before its allotted lifetime is achieved, i.e. failure before reaching the operating time for which the element is designed. Causes of failure include: (1) error in design, manufacturing, assembly and operation; (2) lack of knowledge and experience; (3) insufficient prior testing; and (4) random occurrence despite available knowledge and experience.

We will make the optimistic assumption here that there will be no ‘availability penalty’ for FW/B outage due to scheduled replacement. In this case, only the outage due to unscheduled failures will affect the FW/B availability, A_{wb} , which can then be expressed as:

$$A_{wb} = \frac{MTBF}{MTBF + MTTR} \quad (2)$$

where MTBF is the mean time between failures and MTTR is the mean time to recover from failure. Given a required A_{wb} of 97.8%, we can obtain a relationship between MTBF and MTTR as follows

$$\frac{MTBF}{MTTR} = 43.8 \quad (3)$$

This relationship should serve as ‘an engineering reality check’ for the first wall/blanket design in a fusion system.

The above relationship defines what is required. The next question is what are the achievable MTBF and MTTR? There are presently no data available for fusion systems on failure modes, failure rates, and recovery time. Attempts were made in the literature [8,9,21–23] to extrapolate from current technologies such as fission reactors and Aerospace industries. The most common failure mode is welds. Using average unit failure rates for welds and pipes from fission reactors, and assuming no additional failure modes in the fusion environment (optimistic assumption), values for MTBF can be derived for the first wall/blanket.

Fig. 4 shows the MTBF for the first wall/blanket versus MTTR. The R line shows what is needed, based on Eq. (3). The horizontal line shows what is achievable with current first wall/blanket concepts in current magnetic fusion concepts such as the tokamak. Based on current conceptual designs such as ARIES [24] and ITER [25], MTTR is at least 2–3 months.

The results in Fig. 4 lead to a key conclusion. Current FW/blanket concepts in present magnetic fusion configurations are not capable of meeting the availability requirements because of an expected high failure rate and long down time for recovery from failure.

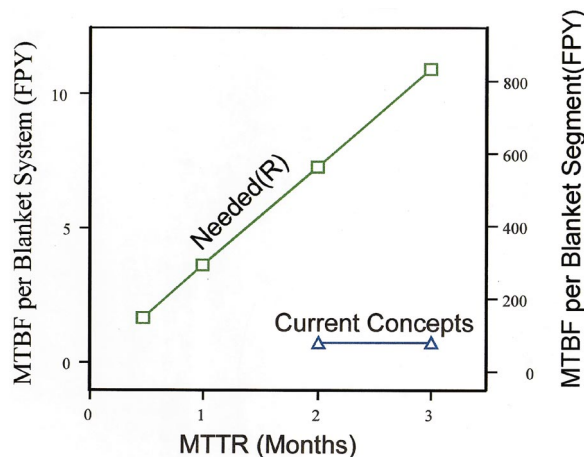


Fig. 4. MTBF versus MTTR for first wall/blanket. The R line shows what is needed. The horizontal line is an estimate of what is achievable with current first wall/blanket concepts in current leading magnetic fusion reactor concepts, assuming 80 segments in the blanket system.

For fusion energy systems to be economically competitive, research must focus on concepts that have a lower failure rate and shorter maintenance time. The failure rate is the product of a unit failure rate, i.e. failure rate per unit area, and the first wall area. Research should seek to develop concepts in which the unit failure rate is inherently lower than that in fission reactors. Also, increasing power density will reduce the first wall area and reduce the failure rate, provided no additional complexity is introduced. Lowering MTTR requires simpler reactor configuration and first wall/blanket concepts for which faster maintenance operations are possible.

2.3. Thermal conversion efficiency

From Fig. 1, the cost of energy is inversely proportional to the thermal conversion efficiency. Since all the thermal energy is produced in the in-vessel system, the conversion efficiency is directly dependent on the temperature of the coolant(s) in the in-vessel system. For ‘bare’ first wall, the temperature of the coolant is limited by the allowable temperature of the structural material (see Table 5).

3. APEX study

Based on results from the previous section, it is clear that current concepts for the in-vessel components (first wall, blanket, divertor, vacuum vessel) will not enable fusion to realize its full potential for economic competitiveness. The APEX study, initiated in 1998, has the following objective:

Identify and explore novel, possibly revolutionary, concepts for the in-vessel components that can substantially improve the vision for an attractive fusion energy system.

Developing a vision for an attractive fusion product must be a joint venture between plasma physics and technology research. For example, realizing high power density requires: (1) confi-

Table 6
APEX primary criteria

-
1. High power density capability
Neutron wall load $> 10 \text{ MW m}^{-2}$
Surface heat flux $> 2 \text{ MW m}^{-2}$
 2. High power conversion efficiency ($> 40\%$ net)
 3. Low failure rates (MTBF > 43 MTTR)
 4. Faster maintenance (MTTR < 0.023 MTBF)
 5. Simpler technological and material constraints
-

nement concepts that can produce high power density; and (2) in-vessel systems that can handle high power density. Similarly, faster maintenance requires an easily accessible confinement configuration as well as a simpler in-vessel system. Therefore, APEX is a part of the overall fusion research effort for innovation and product improvement in both physics and technology.

Concepts explored in APEX must satisfy the functional requirements for the in-vessel system as listed in Table 1. The primary criteria for new innovative concepts are given in Table 6. Capability for handling high power density is a primary driver for the study. Achieving high coolant temperature, and hence high conversion efficiency, is another key criterion. The criteria of low failure rate and fast maintenance are aimed at achieving high availability, as discussed in the previous section. The criterion of simpler technological and material constraints is intended to favor concepts with R&D requirements that have a lower cost and a shorter time scale compared to those of current concepts.

A number of ideas for new innovative concepts have already emerged from the early stages of research in the APEX study. While these ideas need extensive research before they can be formulated into mature design concepts, some of them offer great promise for fundamental improvement in the vision for an attractive fusion energy system.

These ideas fall into two categories. The first category, which may be called revolutionary concepts, seeks to totally eliminate the solid ‘bare’ first wall. An example is a flowing liquid wall concept. A liquid wall has the capability of handling much higher wall loads than a solid first wall. Another example is an all-flowing-liquid

wall and liquid blanket. In addition to the HPD capability, this concept has the potential to satisfy all the other APEX criteria in Table 6, such as low failure rates, faster maintenance, and simpler technological and material constraints.

The second category of ideas focuses on extending the power density capability of current (evolutionary) concepts. An example is the use of high-temperature refractory alloys in the first wall.

Below, we provide a brief description of some of these ideas. We also present some initial analysis of key issues. It is not clear at present if one of these ideas will emerge as a winner or whether other ideas will be discovered. We recognize that innovation and breakthroughs can not be planned. The underlying strategy behind APEX is to provide an environment conducive to innovation.

4. Liquid wall/blanket concepts

A liquid wall followed by a flowing neutronically-thick liquid blanket is an idea that appears to have the highest potential for a very attractive fusion energy system. The major advantages of an all-liquid first wall/blanket system are listed in Table 7.

It must be clearly noted here that the thick liquid Wall/Blanket concept is an idea that, prior to APEX, has not been subjected to extensive analysis and evaluation. A brief history is in order. The idea of using a liquid blanket in a fusion device was first suggested by Christofilos in 1970 [26] for a linear magnetic concept. In this design, the plasma volume was surrounded by a 75 cm thick, free surface lithium blanket flowing at 30 m s^{-1} . Subsequent uses of the liquid walls for magnetic fusion devices are in [27–30].

With regards to the inertial fusion reactors, the first published reactor design concept was a liquid-wall concept proposed by Fraas of ORNL [31]. This design, called BLASCON, features a cavity formed by a vortex in a rotating liquid-lithium pool. Subsequent liquid wall design concepts include a liquid lithium waterfall [32], HYLIFE [33], HYLIFE-I [34], and HYLIFE-II [35].

In all of these concepts, the working liquid must be a lithium-containing medium in order to provide

adequate breeding. The only such practical liquids are lithium, lead–lithium, Flibe, and Sn–Li. Lithium flows (and to a lesser extent, lead–lithium) have strong MHD effects. Flibe does not experience significant MHD forces. Sn–Li was introduced into APEX [40] because it has very low vapor pressure, which makes it particularly suitable for plasma-facing moving liquids. The atomic ratio of tin to lithium will affect the vapor pressure, tritium breeding, and electric conductivity (and hence MHD effects). Analysis and evaluation of Sn–Li is under way. We consider here both lithium and Flibe. A schematic of the concept is shown in Fig. 5. The flow is separated into a fast flowing film, which serves as a first wall, and a slow moving thick liquid flow, which serves as the blanket region. The reason for this separation will be explained shortly.

There are several design ideas being explored in APEX for using liquid first wall and liquid blankets. These include: (1) using liquid only as a ‘convective liquid first wall’ in front of a traditional blanket; (2) using liquid for both the first wall and blanket. In the first case, the convective liquid first wall is ‘formed’ with the aid of a solid back plate. In the second case, i.e. all liquid first wall/blanket, the forces necessary to ‘form’ the liquid into the desired configuration play a fundamental role. Hence, the design ideas can be classified based on the type of forces used. Examples of design ideas for an all liquid FW/blanket

Table 7
Major advantages of an all-liquid first wall/blanket

-
1. Fast flowing liquid in the first wall allows for: (a) very high power density capability; and (b) renewable first wall surface (eliminates erosion as a lifetime limit)
 2. Thick flowing liquid metal blanket will dramatically reduce: (a) radiation damage; and (b) activation in structural materials
 3. Lower unit failure rates, particularly because of elimination of welds in high radiation field region
 4. Easier maintainability of in-vessel components
 5. Improved tritium breeding potential
 6. Applicable to a wide range of confinement schemes
 7. Simpler technological and material constraints
 8. Reduces R&D requirements concerning cost and time scale. Required facilities are simpler and cheaper because it reduces the need for testing in the nuclear environment.
-

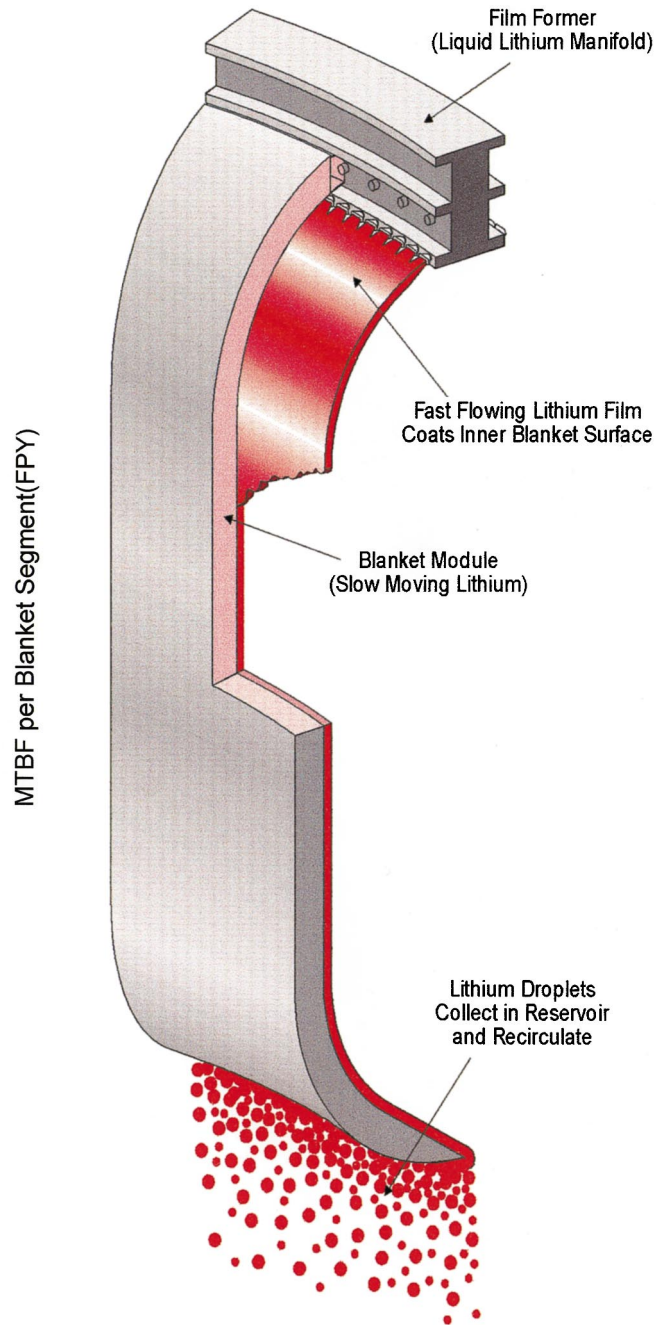


Fig. 5. Conceptual drawing of a liquid wall/liquid blanket/liquid divertor.

are: (a) gravity and momentum driven; (b) swirling flow, i.e. additional rotation force is used; and (c) electromagnetically restrained thick lithium blan-

ket, in which an electromagnetic force is induced in the electrically conducting lithium as the primary mechanism for forming the liquid blanket.

The challenging issues for liquid FW/Blanket concepts are: (1) plasma–liquid interface, particularly the temperature of the liquid free surface facing the plasma; and (2) mechanisms (forces) for forming and maintaining the liquid into the desired geometrical configuration. Some of the key points for these and other issues are briefly analyzed below.

As an aid in facilitating the discussion below, Fig. 5 shows a schematic of a particular design idea of the liquid wall/blanket/liquid divertor. In this particular figure, a fast flowing liquid jet ($\sim 1\text{--}2$ cm) serves as the first wall facing the plasma. Behind the liquid wall is a slowly moving thick liquid region that serves as a liquid blanket. The liquid flows to the bottom and naturally forms a liquid divertor.

4.1. Liquid surface temperature

Since the liquid surface is directly exposed to the plasma, the plasma–liquid interactions are very important for all liquid wall and liquid wall/blanket concepts. Concerns about impurity transport to the plasma will set a limit on the amount of material allowed to evaporate or sputter from the liquid surfaces, possibly as a function of poloidal location around the plasma. This evaporation limit will in turn give a surface temperature limit of the flowing liquid. Such limits will have to be derived from sophisticated plasma-edge modelling code. Such effort is underway. On the other hand, the temperature profile of the liquid surface can be readily calculated as a function of heat loads and flow parameters, as shown below. Relevant details are given in [36].

The thermal response of the liquid surface depends strongly on the heat load from plasma radiation and is not very sensitive to nuclear heat generation by neutrons. In previous studies, plasma radiation was assumed to be deposited at the first wall surface (i.e. a purely surface head load). In this work, we find that accounting for the plasma radiation (Bremsstrahlung) spectrum is important for accurate calculation of the liquid surface temperature.

The attenuation length of 10 keV mono-energetic X-rays in Li, Flibe, and $\text{Li}_{17}\text{Pb}_{83}$ is \sim

1.3×10^5 , ~ 1000 , and ~ 10 μ , respectively (i.e. the attenuation coefficient of Li is ~ 2 orders of magnitude lower than Flibe, whereas the attenuation coefficient of Flibe is $\sim 1\text{--}2$ orders of magnitude lower than $\text{Li}_{17}\text{Pb}_{83}$, see Fig. 6). Thus, surface wall load could, in principle, be deposited volumetrically over a measurable depth in the convective layer of Li and to a lesser extent in Flibe while it is deposited at the surface in the case of $\text{Li}_{17}\text{Pb}_{83}$ due to its high attenuation coefficient. The incident X-rays consist mainly of Bremsstrahlung spectrum and line radiation from impurities and cover a wide range of energies in the eV–keV range. Classical Brem. Radiation was considered at various electron temperature, Te. For 10 keV Brem. Radiation of 1 MW m^{-2} , the heat deposition rate (HDR) at the surface is $\sim 9 \times 10^4 \text{ w cc}^{-1}$ in Li and $5 \times 10^5 \text{ w cc}^{-1}$ in Flibe (Fig. 7). These large values are due to the absorption of low-energy tail of the Brem. spectrum below 80 eV in Li and ~ 200 eV in Flibe whose attenuation length is a fraction of a micron. This fraction of the spectrum is ~ 0.4 and 2%, respectively. At the bulk of the layer, lower HDR is attainable at measurable depth. For example, at a 1 cm depth, the HDR is $\sim 10 \text{ w cc}^{-1}$ (Li) and 8 w cc^{-1} (Flibe). For a HDR of $\sim 50\text{--}60 \text{ w cc}^{-1}$ (which is comparable to neutrons/gamma heating at 7 MW m^{-2} NWL), the depth for Te = 10 keV is ~ 0.1 cm (Li) and ~ 0.2 cm (Flibe). This suggests that part of the surface load is considered to be deposited volumetrically. This has an impact on the temperature of the liquid at the surface as shown below.

The temperature profile of the liquid wall is calculated using a three-dimensional finite difference heat transfer code under a combined surface heat load of 2 MW m^{-2} and NWL of 10 MW m^{-2} . The code takes the velocity profile as an input parameter and calculates the temperature distribution in the fluid. In the calculation, the surface heat flux is either accounted as a boundary condition in cases where X-ray penetration is insignificant or as an internal heat source. The surface and bulk temperature distributions as fluids proceed downstream are shown in Figs. 8 and 9 for lithium and Flibe jets, respectively. As shown, accounting for X-ray penetration significantly reduces the jet surface temperature, partic-

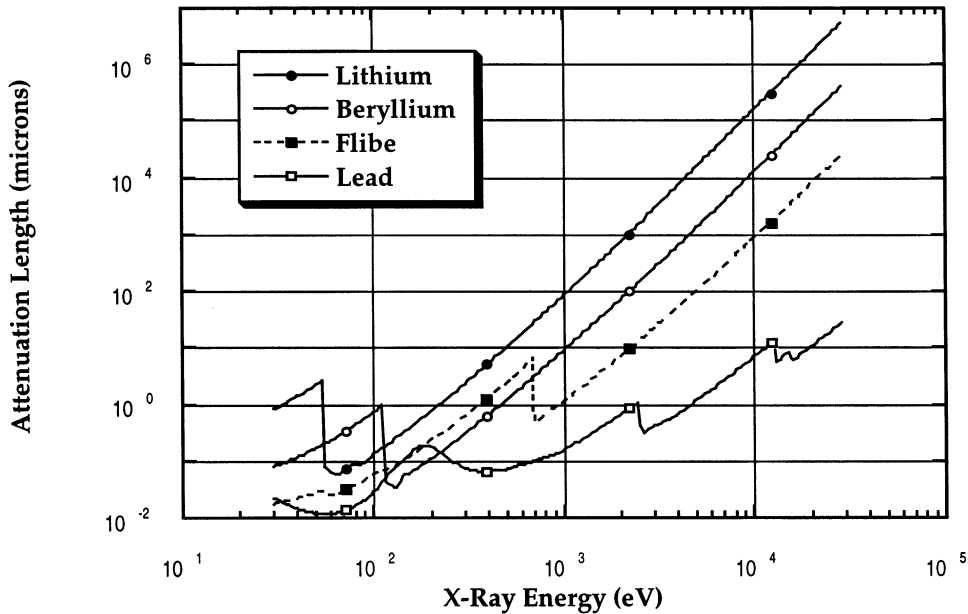


Fig. 6. Attenuation length of X-rays in Lithium, Beryllium, Flibe, Lead, and $\text{Li}_{17}\text{Pb}_{83}$ vs. photon energy.

ularly in the case where the Flibe surface is exposed to a hard Bremsstrahlung radiation spectrum (for example as the case shown: a classical Bremsstrahlung radiation spectrum corresponding to an average T_e of 10 keV). Nevertheless, most of the Bremsstrahlung radiation is deposited within the first one cm of the jet. The peak surface temperatures as shown for the 1-cm-thick lithium and Flibe jets under the hard Bremsstrahlung radiation heating are 327 and 743°C, respectively, with corresponding evaporation rates of 10^{19} and 10^{23} atoms $\text{m}^{-2} \text{s}^{-1}$. It is expected that the Flibe jet surface temperature can be reduced further by turbulent eddies. Whether these temperatures are acceptable or not is yet to be determined from detailed plasma-edge modelling and calculations.

4.2. Innovative schemes for plasma–liquid interactions

As mentioned previously, the compatibility of free-surface liquids with plasma operation is a key requirement. In order to reduce impurity transport to the plasma, the amount of material allowed to evaporate (or sputter) from the liquid

surface must be reduced to an acceptable level.

Several innovative schemes have been proposed and are being explored in APEX to assure compatibility of free-surface liquids with plasma operation. These include:

1. Design innovation

Through proper design ideas, the temperature of the free-surface liquid can be controlled to an

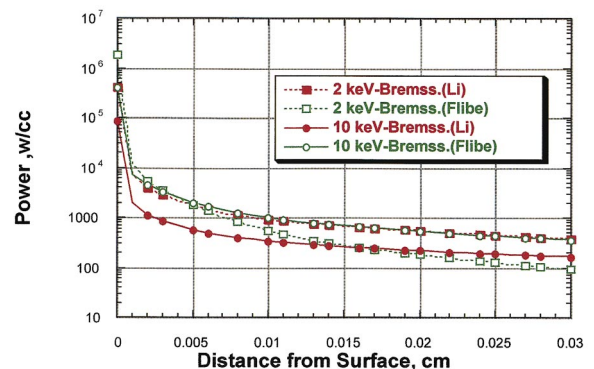


Fig. 7. Power deposition rate from 1 MW m^{-2} surface wall load in Li and flibe convective layer (classical Bremsstrahlung spectrum)—depth 0.03 cm. Results are shown for two values of the electron temperatures, i.e. 2 and 10 KeV.

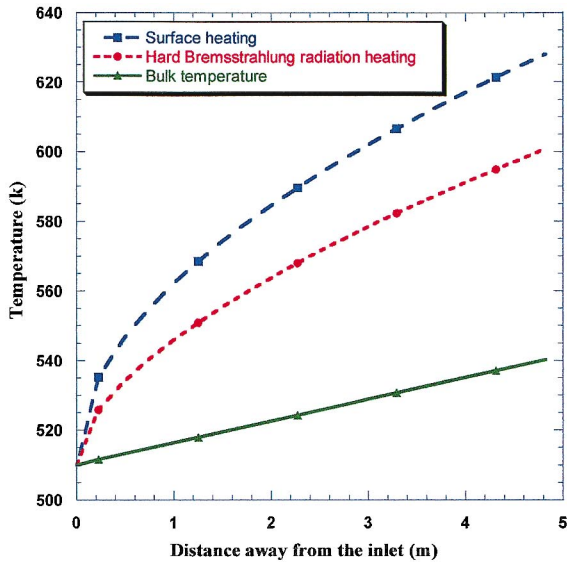


Fig. 8

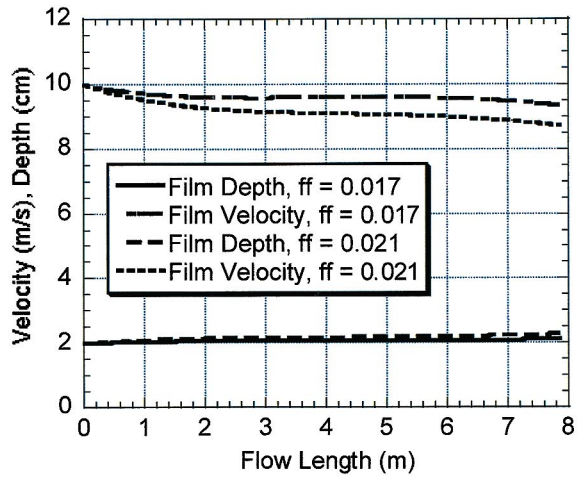


Fig. 10

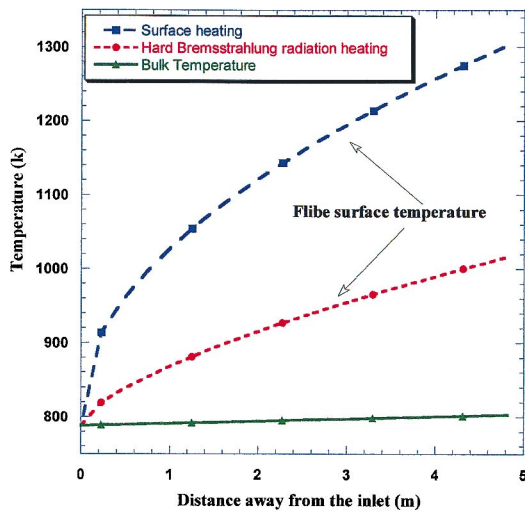


Fig. 9

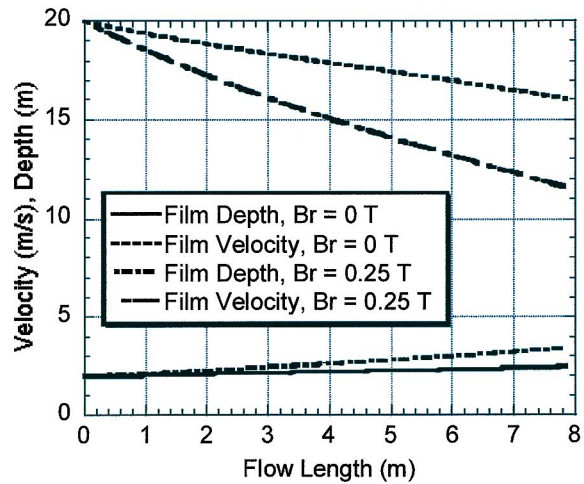


Fig. 11

Fig. 8. Lithium jet surface and bulk temperatures as jet proceeds downstream (For operating conditions of a surface heat load of 2 MW m^{-2} combined with a neutron wall load of 10 MW m^{-2} and the jet velocity $= 20 \text{ m s}^{-1}$).

Fig. 9. Flibe jet surface and bulk temperatures as jet proceeds downstream (For operating conditions of a surface heat load $= 2 \text{ MW m}^{-2}$ combined with a neutron wall load $= 10 \text{ MW m}^{-2}$ and jet velocity $= 20 \text{ m s}^{-1}$).

Fig. 10. Flow profiles for flibe film on an 8 m cylindrical surface with various friction factors.

Fig. 11. Flow profiles for lithium film on an 8 m cylindrical surface with 7 T toroidal field and various radial field strengths.

acceptable level. Examples include: (a) Dividing the thick liquid first wall/blanket into two regions. In the first region, facing the plasma, a thin (~ 1

cm) liquid jet flows at relatively high enough velocity to keep the surface temperature sufficiently low under the intense surface heating from

plasma radiation (and the smaller bulk heating from neutrons). In the second region behind the fast jet, thick liquid flows at sufficiently low speed to keep the liquid temperature high enough to achieve the desired high thermal efficiency. Analysis shows that this approach is sufficient for lithium, and tin–lithium to assure compatibility with plasma operation. For flibe, this scheme may or may not be sufficient depending on the surface heat transfer; and (b) new schemes to enhance heat transfer at the liquid free surface by promoting controlled surface mixing and wave formation to eliminate or broaden the surface thermal boundary layer.

2. Material innovation

Tin–lithium has been proposed [40] as the breeding/coolant liquid because it has a very low vapor pressure even at elevated temperatures. Calculations show that the free-surface liquid temperature for Sn–Li may be allowed to be as high as 800°C. However, Sn–Li has less favorable heat transfer characteristics than lithium and more pronounced MHD effects than flibe. Analysis to quantify the real potential of this promising material is underway.

3. Rigorous analysis

Analysis to date shows that the exact value of the liquid free-surface temperature is sensitive to many parameters and phenomena. Therefore, many commonly used assumptions are generally not satisfactory. An example was shown in the previous section where accurate treatment of the penetration of Bremsstrahlung radiation yielded substantially lower temperatures compared to those obtained with the commonly used assumption of delta function surface heating. Another example is the need for detailed hydrodynamics and heat transfer calculations for the free-surface liquid.

4.3. Convective liquid layer wall

A minimal use of free-surface liquid concept is to flow a fast moving (convective), thin liquid layer on the inside (i.e. on the plasma side) of a structural first wall. The layer adheres to the curved wall by means of its centrifugal acceleration V^2/R . The thin layer is easier to control than

thick liquid blankets. It provides high heat flux removal capability, and a renewable liquid surface immune to radiation damage. It eliminates thermal stress as a limiting factor in the structural first wall. The liquid film can also be used at the bottom of the reactor as an integrated liquid surface divertor, and then removed from the vacuum by gravity drainage, or an E M pump (if the working liquid is an electrical conductor). Behind the liquid wall and structural first wall, any of the conventional blankets can be used. The design for this concept is similar to the fast flowing film in Fig. 5 with the blanket module behind it having a solid structural first wall.

The liquid wall concept satisfies mainly the first of the APEX Primary Criteria of Table 6, i.e. high power density removal capability. It will also cause a modest reduction in the unit failure rate. However, it will do little to reduce radiation damage in the structure or to facilitate faster maintenance.

A key issue for this convective liquid layer concept concerns the characteristics of the flow on a concave substrate surface that produces shear and whether this kind of flow can be established and maintained in the reactor environment. In order to produce a compact flow trajectory parallel to plasma contour lines, the flow has to carry adequate centrifugal inertia against the gravity, friction, and MHD forces.

The results of hydraulic calculations are shown in Fig. 10 for Flibe and Fig. 11 for lithium. The upper two lines in each figure are for flow velocity (m s^{-1}) and the lower two lines are for the flow depth (cm). In both figures, the horizontal axis is the flow length starting at the top of the reactor and proceeding downward along the concave structural substrate. The calculations for lithium include a simple correlation for MHD forces, and assume an electrically insulated backing wall. As seen in Figs. 10 and 11, the friction on the back plate dominates the hydraulic calculations for the velocity/depth of the convective liquid layer. The calculations indicate the possibility that fast, thin flows can indeed be established and maintained on a curved backing wall. Flow depth equilibria of ~ 2 cm appear achievable for both lithium and Flibe. The turbulent Flibe flow is seen to be

constant over the required flow length, even after a 25% increase in the friction factor over that expected for a smooth wall. An initial speed of 10 m s^{-1} is sufficient to ensure the Flibe layer remains adhered over the entire inverted flow length. The laminar-MHD lithium flow, however, is very sensitive to the presence of any radial magnetic field component (normal to the liquid free surface). Due to the laminar heat transfer at the free surface, lithium also requires a greater flow velocity than Flibe to mitigate the temperature rise at the free surface. However, for a flow along a flux surface ($B_R = 0$), a 20 m s^{-1} velocity can be maintained over the majority of the flow length, with minimal thickening for the film. Multidimensional effects and reaction to time varying magnetic and electric fields have not yet been investigated, and remain to be addressed in more detailed modelling.

4.4. Thick liquid wall/blanket

As discussed earlier using a neutronicly-thick liquid first-wall and blanket with little or no structure has tremendous advantages. There are a number of key issues that must be addressed before the idea can be evolved into a practical concept. One of the most fundamental issues is how to form, establish, and maintain such a thick liquid flow in a specified reactor configuration. Three approaches were considered: (a) swirling flow, or mechanical-force driven rotating flow as proposed in [29]; (b) gravity- and momentum-driven (GMD) flow; and (c) electromagnetically-restrained lithium flow as proposed in [37].

The most exciting results to date have been obtained for an all-liquid first wall/blanket with a swirling flow in the Field Reversed Configuration (FRC) confinement scheme. Numerical hydrodynamic analysis performed using a commercially available code Flow 3D (a 3-D time-dependent Navier Stokes Equations solver with a volume of fluid free surface tracking algorithm) shows the feasibility of forming and maintaining an all liquid swirling liquid FW/blanket with a uniform thickness. High azimuthal and axial velocities with a thick liquid FW/blanket (thickness $> 50 \text{ cm}$) results in a high Reynolds number flow both

in the axial and azimuthal flow. The concept is shown in Fig. 12.

Below, we will analyze the required thickness for liquid blankets, then we will discuss key aspects of other (no swirling) schemes for forming liquid blankets.

4.4.1. Required thickness for liquid blanket

A primary motivation for considering a thick liquid blanket is to protect the structure behind it from radiation damage and from becoming highly activated. It is, therefore, important to evaluate the neutronics response of the structural material as a function of the thickness of the liquid blanket protecting it [36].

Flibe is a more powerful material in attenuating high-energy neutrons due to inelastic scattering in Fluorine and (n, 2n) reactions in beryllium. Lithium, on the other hand, is a good moderator for both high-energy and low-energy neutrons through inelastic scattering in Li-7 and absorption in Li-6. The impact of increasing the liquid thickness on the DPA, and helium production rates in the structure behind the liquid, is shown in Figs. 13 and 14, respectively for 7 MW m^{-2} wall load. The variation of the maximum ratio of the He:DPA ratio with the liquid layer thickness is shown in Fig. 15.

For a bare wall, the ratio is ~ 11 in Flibe/(Flibe-FS) system and 3.2 in the Li/(Li- $\text{V}_4\text{Cr}_4\text{Ti}$) system. At $L = 50 \text{ cm}$, this ratio drops to the values of 6.2 and 1.5, respectively.

These results show that substantial reduction in the radiation damage of the structural material can be obtained with moderate thickness of Flibe. With 50 cm of Flibe, the helium production and DPA are reduced by a factor of ~ 80 . This allows the candidate structural materials to last for the whole plant lifetime. It actually appears that 30 cm of Flibe may be adequate for this purpose. However, thicker layers will be required with lithium. It should be noted that any thickness of liquid will prolong the lifetime of the structure.

4.4.2. Gravity- and momentum-driven (GMD) liquid blanket

The simplest approach that can be conceived for a thick liquid blanket is free falling jets under

the effect of gravitational force with the initial direction of the jets controlled by inlet momentum. The liquid first wall must be separated from the liquid blanket. As shown earlier, the liquid wall will have high velocity to remove the high surface heat flux while keeping the temperature of the liquid surface facing the plasma low. The liquid blanket flow must be at a lower velocity in order to achieve high temperature and to reduce pumping power requirements. Detailed calculations are given in [36].

2-D free-surface fluid flow calculations for Flibe were performed using the RIPPLE code (35). Fig. 16 shows the Flibe jet thickness as a function of distance along the jet path. The results are shown for various values of the initial velocity. Under free fall conditions, the law of mass conservation results in jet thinning as the jet proceeds downstream due to the gravitational forces. As shown in Fig. 16, at low initial velocity the jet thickness is rapidly reduced from an initial 10 to 2 cm at 2 m downstream. This jet thinning is a serious issue because it opens void gaps through which radiation will stream through and reach the structure

behind the thick liquid blanket. Therefore, jet thinning is a key issue that casts doubts on the practicality of a gravity-driven liquid blanket.

The jet thinning effect can, in principle, be reduced or nearly eliminated by increasing the initial velocity to a point where gravity acceleration effects are small compared to the initial momentum. However, this requires high velocities. For example, in Fig. 16, there is still a 50% reduction in the area along a 4-m path for an initial velocity of 7 m s^{-1} . A further increase in the initial velocity raises concerns about the pumping power. It is calculated that 30-cm-thick Flibe blanket would require a pumping power of $\sim 6\%$ of the thermal power at an initial jet velocity of 7 m s^{-1} .

Several possibilities can be thought of to overcome the jet thinning problem. For example, several separately flowing jets can be injected at various vertical locations and staggered enough to provide the radiation protection function. However, this leads to configuration complexity, which a liquid blanket is supposed to avoid. Much more investigation and analysis are required in this area.

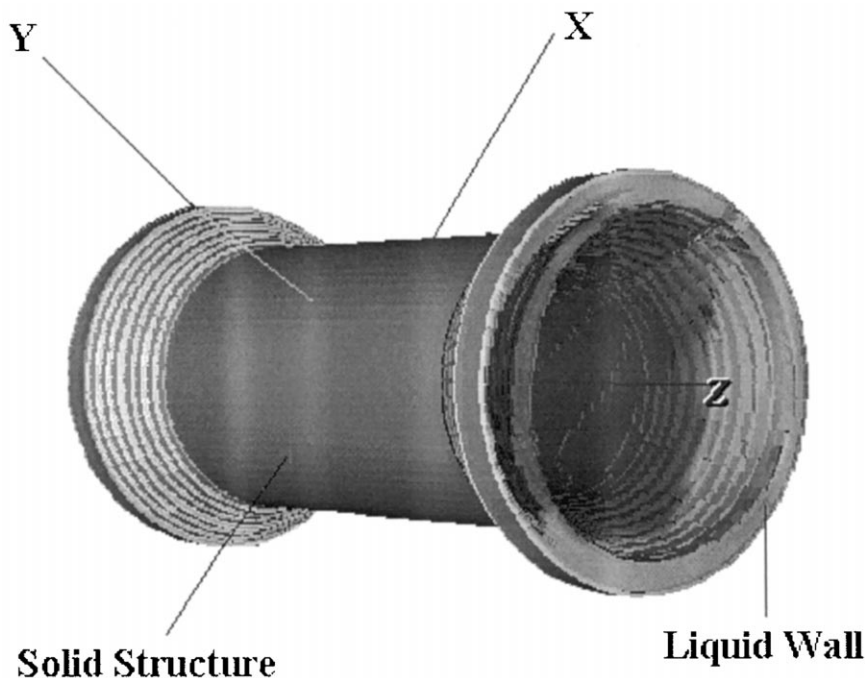


Fig. 12. Swirling flow for an all liquid first wall/blanket in FRC confinement configuration.

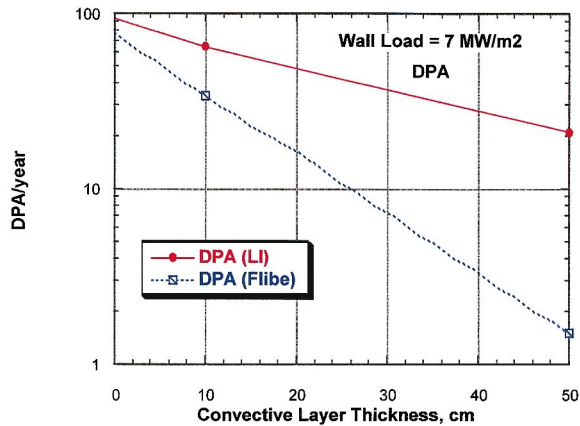


Fig. 13

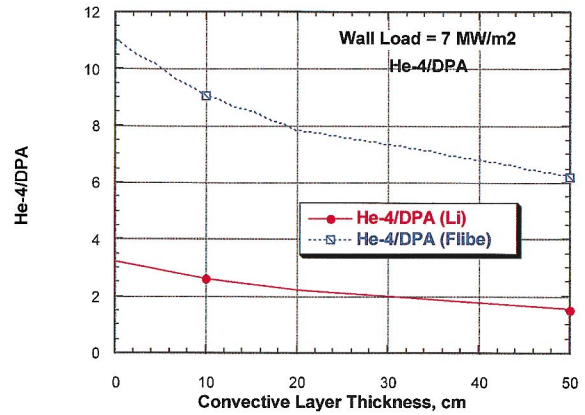


Fig. 15

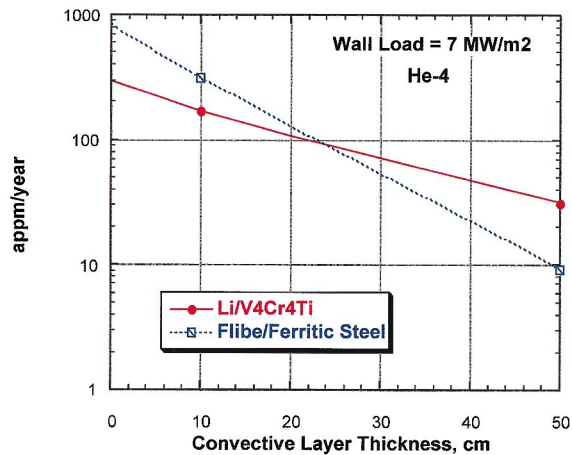


Fig. 14

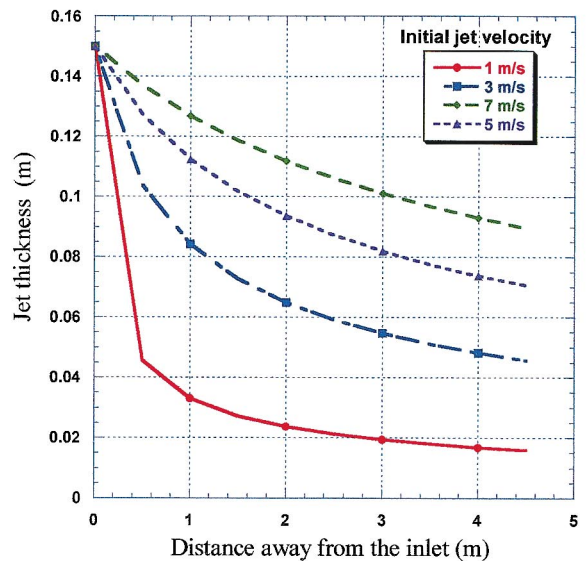


Fig. 16

Fig. 13. Impact of increasing the liquid blanket thickness on the maximum DPA rate at the vacuum vessel (wall load = 7 MW m^{-2}).

Fig. 14. Impact of increasing the liquid blanket thickness on the maximum helium production rate at the vacuum vessel (wall load = 7 MW m^{-2}).

Fig. 15. Variation of He:DPA ratio as a function of liquid wall/blanket thickness for lithium and flibe.

Fig. 16. Flibe jet thickness as a function of distance away from inlet for various values of initial velocity. (JET thickness is reduced as JET proceeds downstream due to gravitational force).

4.4.3. Pocket GMD liquid blanket

This concept has been proposed in APEX as a modification to the GMD liquid blanket in an advanced tokamak configuration. As shown in the previous section, the GDM concept suffers from jet thinning when no structure is used. The Pocket

GMD (PGMD) concept attempts to use some structural materials to aid in establishing and maintaining the liquid blanket.

The concept has two main sections. The front section, facing the plasma, has a high velocity ($> 10 \text{ m s}^{-1}$), thin ($< 2 \text{ cm}$) liquid jet flowing in

the poloidal direction. The second section has a series of fluid compartments along the poloidal and toroidal direction as shown in Fig. 17.

Initial calculations using the FLOW 3-D code with Flibe show excellent promise. The flow characteristics and design parameters obtained show that this concept has an excellent potential to satisfy many of the APEX primary criteria. The main disadvantage of this PGDM concept relative to a purely liquid blanket is the use of a structural material to form the boundary of the fluid compartments. This disadvantage can be reduced by minimizing the amount of structural material used and by developing a clever scheme for supporting such a structure.

4.4.4. Electromagnetically restrained lithium blanket

In this concept, liquid lithium flows into the vacuum vessel at the top in two electrically separated axisymmetric thick streams, one inboard and one outboard of an axisymmetric insulating break in the vacuum vessel. The lithium inflow is from ducts giving it an initial radial velocity, with one stream directed inwards and the other directed outwards. The two streams flow to the bottom of the vacuum vessel and then flow out through axisymmetric exit ducts. The vacuum vessel is shaped in conformance with the shape of the designed reactor plasma, so that lithium flows along poloidal field flux lines. DC electric current

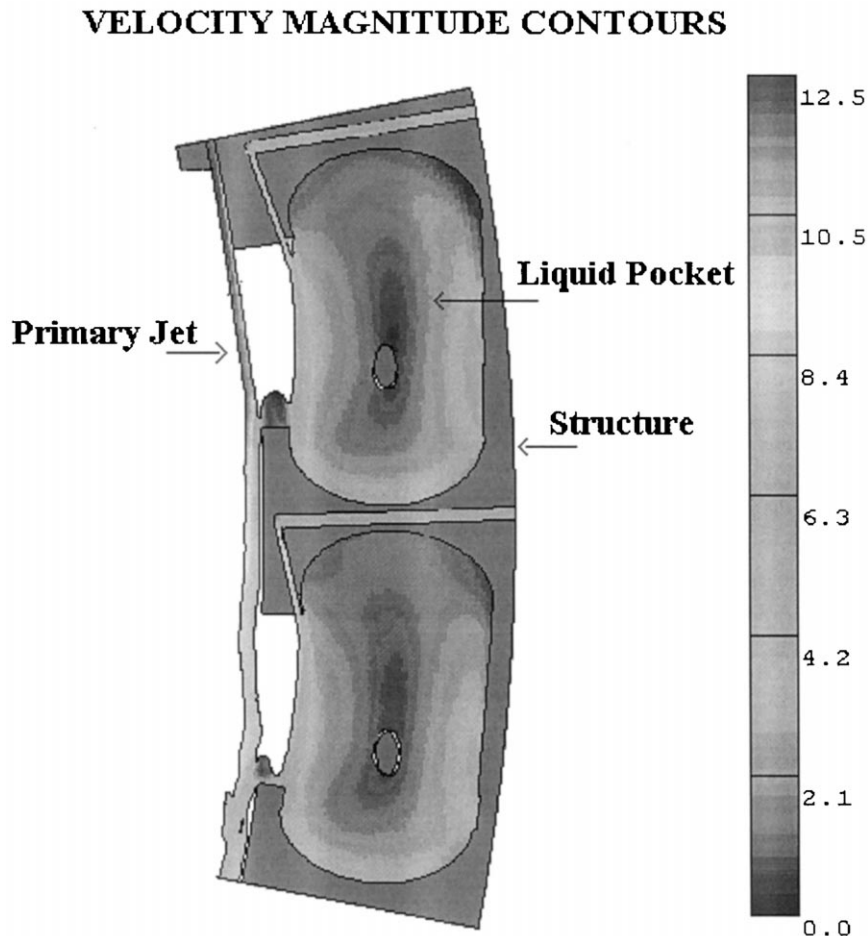


Fig. 17. Illustration of pocket GMD liquid wall/liquid blanket in two adjacent compartments.

from an external power supply is galvanically injected into each stream and flows into the lithium parallel to the TF current in the nearby TF electromagnets, thus providing a $J \times B$ force density which helps centrifugal force in pushing the lithium streams away from the plasma and against the vacuum vessel walls.

This concept was proposed by Woolley [37] for tokamaks but it can be applied to other confinement schemes. The electromagnetic interactions with this concept in magnetic confinement systems are complex and require new model development to permit design concept analysis. Such model development is underway.

5. Other concepts

5.1. Gravitational flowing Li_2O particulates

This concept is similar to the ones discussed earlier. Instead of using a liquid layer as the breeding and heat removal material, this concept selects a gravitation flow of Li_2O . Li_2O is selected due to its high breeding potential, low vapor pressure at high temperature, and low activation. The concept is shown in Fig. 18. The Li_2O enters the upper blanket region between the magnets by gravitation flow. Upon entering the blanket region, the flow of Li_2O is diverted toward the outer and inner blanket region by a baffle. After it reaches the blanket region, it flows downward by the gravitational force. The first layer of Li_2O flow, ~ 3 cm thick, will flow unrestricted to remove the surface heat. The rest of the Li_2O will be restricted within a SiC structure. The SiC zone will have different openings at the bottom of the flow channel to control the flow velocity of the Li_2O . The front region will have a higher velocity than the back, so that the Li_2O will exit from the blanket with a reasonably uniform temperature. The Li_2O particulates will exit from the blanket by gravitational force, and will be moved upward by a mechanical conveyor. They will drop down (also by gravitation force) through a heat exchanger to transfer the heat to a helium gas, and will be moved upward again by another mechanical converter, ready to be dropped into the blanket again.

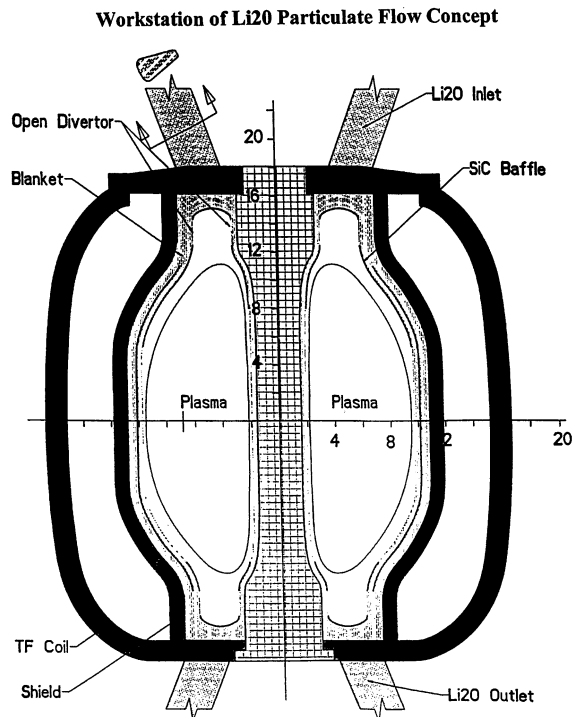


Fig. 18. Workstation of Li_2O particulate flow concept

The key difference between this concept and the previously discussed liquid wall concepts is the much lower vapor pressure of Li_2O . Therefore, the Li_2O coolant has the potential to go to a very high temperature. The vapor pressure of Li_2O reaches only 10 (-5) torr at 1000°C . This very low vapor pressure significantly increases the temperature design window of this concept. Also, since the Li_2O is a non-conductor, there is no MHD effect involved in this concept.

There are many problems with this concept that will require further analysis and modification. A key issue is particle flow dynamics and control. The current idea uses baffles to control the Li_2O flow in the high radiation environment. These baffles represent a major issue because they are exposed directly to the surface heat flux and may require active cooling. They also will need to be replaced in short intervals. A combination of particle flow dynamics and heat transfer analysis is planned to assess the feasibility and attractiveness of this concept. Another key issue is the difficulty of the design for a particulates-to-solid wall heat exchanger.

5.2. Helium-cooled high temperature refractory alloys

This concept is an example of an attempt to extend the limits of current evolutionary concepts in order to handle high power density at the first wall. As shown earlier, high-temperature refractory alloys such as tungsten, T111, TZM, and Nb–1Zr can handle much higher wall loads than the low activation materials.

In this concept, a high pressure (18 MPa) helium coolant is used in a high-temperature refractory alloy first wall. However, calculations [38] show that satisfying the APEX criteria of 10 and 2 MW m⁻² surface heat flux requires reducing the thickness of the first wall to 3 mm. In the blanket, helium coolant is used with a liquid lithium or LiPb breeder. Because of the lower power density in the blanket, the use of low activation structural material is possible.

Compared to current evolutionary concepts, this concept allows HPD capability. However, most of the other issues remain the same. In particular, the failure rate at the first wall may be too high to permit achievement of high availability. Further evaluations and analysis of the concept are planned.

6. Conclusions

Current concepts for fusion energy systems will have clear environmental and safety advantages. However, developing a vision for an economically competitive fusion energy system remains the grand challenge for fusion researchers. The FPT, which consists primarily of the in-vessel components (first wall, blanket and divertor), plays a most critical role in determining the economic potential of fusion systems.

Current world wide concepts for the ‘in-vessel’ components will not enable fusion to realize its full potential for economic competitiveness. Analysis shows that the limitations of the current concepts are most serious in the following areas:

1. Low power density capability

Solid first walls have been shown to have low wall load and surface heat flux capabilities, mostly

because of thermal stress limits. Low activation materials, ferritic steel, vanadium alloys and SiC–SiC composites are limited to peak NWL of 1.5, 3.2, and 2.5 MW m⁻², respectively. The average NWL is lower than the peak wall load by a factor, typically, of ~1.4. Such low wall loads result in a fusion system power density that is more than two orders of magnitude lower than that in PWR and LMFBR.

It should be noted that some reactor studies are based on wall load limits that are up to ~50% higher than those obtained in this work. Some of the reasons for such higher values is that reactor studies generally assumed thinner first walls, negligible first wall erosion, and a smaller fraction of the alpha power radiated to the first wall. Even if the values of reactor studies, i.e. 50% higher wall load limits, are accepted, the corresponding power density still remains drastically lower than that in fission reactors.

High-temperature refractory alloys offer higher wall load capability but they do not meet the low long-term activation criterion. The peak NWL limits for Nb–1Zr, tungsten, TZM, and T111 as first wall structural materials are calculated as 6.6, 8.8, 13, and 11.6 MW m⁻², respectively. While these values are substantially higher than those obtained with low activation materials, they are still relatively low compared to what fission reactors can achieve.

It should also be noted that current blanket concepts have serious limitations on the power density that appear to be comparable to those in the solid first wall. Such limitations arise, for example, from temperature limits and poor thermal conductivity of solid breeder ceramics, and limitations on flow speed imposed by MHD effects in flowing liquid metals. The limitations on the power density in the blanket behind the first wall have not been addressed in this paper but there is ample relevant information in the literature. Ref. [39] provides a summary of such limitations.

2. Low temperature capability

The low-activation structural materials commonly used in the first wall are limited in the maximum temperature capability for a variety of reasons. For example, ferritic steel and V–Cr–Ti

have maximum practical operating temperature limits of 550 and 700°C, respectively. The corresponding peak coolant temperatures, and hence the thermal conversion efficiency are relatively low. High-temperature refractory alloys have a potential to enable much higher thermal conversion efficiency.

3. Short MTBF, long MTTR, and low availability

It has been shown in this work that in order to obtain a reasonable overall fusion system availability the relationship $MTBF \geq 43.8 MTTR$ must be satisfied by the first wall/blanket (FW/B) system. Current concepts fail to satisfy this criterion. MTTR is generally greater than 2–3 months for current FW/B concepts in the leading confinement schemes such as the tokamaks. Based on extrapolation from current fission, aerospace and other technologies, MTBF for current FW/B concepts are likely to be < 12 months.

Because of the limitations summarized above for current in-vessel components concepts, the APEX study was initiated. The objective of APEX is to ‘identify and explore novel, possibly revolutionary concepts for the in-vessel components that can substantially improve the vision for an attractive fusion energy system’. A number of criteria for attractiveness have been identified.

A number of ideas for new innovative concepts have already emerged from the early stages of research in the APEX study. These ideas fall into two categories. The first category, called revolutionary concepts, seeks to totally eliminate the solid ‘bare’ first wall. An example is a flowing liquid wall concept. A liquid wall has the capability of handling much higher wall loads, e.g. 30 MW m⁻², than a solid first wall. Another example is an all-flowing-liquid wall and liquid blanket. In addition to the high power density capability, this concept has the potential to have higher temperature, lower activation, lower failure rate, faster maintenance, and simpler material and technological constraints than current concepts. The second category of ideas, called evolutionary concepts, focuses on extending the power density capability of current concepts. An example is the use of high-temperature refractory alloys in the first wall.

Analysis of the new innovative ideas reveals a number of challenging engineering science issues that offer excellent opportunities for exciting research in fusion technology. Therefore, extensive research on these innovative ideas has the promise of: (1) providing a new vision for more attractive fusion energy systems; (2) enriching many areas of engineering sciences; and (3) providing a greater link between research on fusion and research in other fields.

Acknowledgements

I would like to thank all members of the APEX Team for their great efforts and dedication to this important study. Special thanks are due to my colleagues Drs Alice Ying, Anter El-Azab, Mahmoud Youssef, Karani Gulec, and Neil Morley of UCLA, to Dr Dai-kai Sze from ANL, Dr Robert Woolley from PPPL, Dr Clement Wong from GA and Dr S. Malang from FZK for their valuable contributions to many parts of the study. Very special thanks are due Sam Berk from the U.S. Department of Energy. His vision and deep understanding of fusion technology issues were key to initiating APEX and formulating its direction and approach.

References

- [1] J.P. Holden, Safety and environmental aspects of fusion energy, *Annu. Rev. Energy Environ.* 16 (1991) 235–258.
- [2] J. Raeder, et al., Safety and Environmental Assessment of Fusion Power (SEAFP), EURFUBRU XII-217/95, Brussels: European Commission, 1996.
- [3] R.L. Miller, Fusion power plant economics, *Fusion Technol.* 30 (3) (1996) 1599–1604.
- [4] R.L. Miller, Economic goals and requirements for competitive fusion energy, *Proceedings of ISFNT-4*, 6–11 April, 1997, Tokyo, *Fusion Eng. Des.* 41 (1998) 393–400.
- [5] T.C. Hender, P.J. Knight, I. Cook, Key issues for the economic viability of magnetic fusion power, *Fus. Technol.* 30 (3) (1996) 1605–1612.
- [6] M.A. Abdou, S.E. Berk, A. Ying, et al., Results of an international study on a high-volume plasma-based neutron source for fusion blanket development, *Fus. Technol.* 29 (1996) 1–57.
- [7] M.A. Abdou, Blanket Comparison and Selection Study—Interim Report, Argonne National Laboratory,

- ANL-FPP-83-1, 1983; see also final report ANL/FPP-84-1, 1984.
- [8] S. Malang, M.S. Tillack (Eds.), Development of Self-Cooled Liquid Metal Breeder Blanket, FZKA-5581, Forschungszentrum Karlsruhe, November, 1995.
- [9] M. Dalle Donne, Development of EU helium-cooled pebble bed blanket, ISFNT-4, Tokyo, 1997, Fusion Eng. Des., in press.
- [10] L. Giancarli G. Benamati, M. Fufferer, G. Marbach, C. Nardi, J. Reimann, Development of EU water-cooled Pb–17Li blanket, Fusion Eng. Des., in press.
- [11] M.A. Abdou, P.J. Gierszewski, M.S. Tillack, et al., Technical issues and requirements of experiments and facilities for fusion nuclear technology, Nucl. Fusion 27 (4) (1987) 619.
- [12] H. Takatsu, H. Kawamura, S. Tanaka, Development of ceramic breeder blankets in Japan, ISFNT-4, Tokyo, 1997, Fusion Eng. Des., in press.
- [13] S.J. Zinkle, Materials Selection Issues for High Wall Loading Concepts, Presented during the APEX Study Meeting, 15–17 October, 1997, University of California, LA (full text available at <http://www.fusion.ucla.edu>).
- [14] S.J. Zinkle, A. El-Azab, Structural Materials Database and Operating Temperature Limits, Presented during the APEX Study Meeting, 12–14 January, 1998, University of California, LA (full text available at <http://www.fusion.ucla.edu>).
- [15] S.J. Zinkle, N.M. Ghoniem, Status of Recent Activities by the APEX Materials Group and Chemical Compatibility and Radiation Effects Issues in High Temperature Refractory Metals, Presented during the APEX Study Meeting, 6–8 May, 1998, University of California, LA (full text available at <http://www.fusion.ucla.edu>).
- [16] N.M. Ghoniem, Assessment of High Temperature Refractory Metals, Presented during the APEX Study Meeting, 6–8 May, 1998, University of California, LA (full text available at <http://www.fusion.ucla.edu>).
- [17] A. El-Azab, NWL Limits for Some Refractory Materials, Presented during the APEX Study Meeting, 6–8 May, 1998, University of California, LA (full text available at <http://www.fusion.ucla.edu>).
- [18] Aerospace Structural Metals Handbook, 1992 ed., vol. 5, in: William F. Brown, Jr., Harold Mindlin, C.Y. Ho (Eds.), CINDAS, Purdue University.
- [19] S. Majumdar, R. Mattas, Evaluation of Structural Limits, Presented during the APEX Study Meeting, 12–14 January, 1998, University of California, LA (full text available at <http://www.fusion.ucla.edu>).
- [20] A. El-Azab, N.M. Ghoniem, Viscoelastic analysis of mismatch stresses in ceramic matrix composites under high-temperature neutron irradiation, Mech. Mater. 20 (1995) 291.
- [21] M. Abdou, A volumetric neutron sources for fusion nuclear technology testing and development, Fusion Eng. Des. 27 (1995) 111–153.
- [22] R. Bunde, S. Fabritsiev, V. Rybin, Reliability of welds and brazed joints in blankets and its influence on availability, Fusion Eng. Des. 16 (1991) 59–72.
- [23] A. Ying, M. Abdou, Application of reliability analysis methods to fusion components testing, Fusion Eng. Des. 27 (1995) 191–197.
- [24] F. Najamabadi and the ARIES Team, Overview of the ARIES-RS reversed–shear tokamak power plant, Fusion Eng. Des. 38 (1997) 3–25.
- [25] R. Aymar, Final Conceptual Design Report, to be published as IAEA Report, 1998.
- [26] N.C. Christofilos, A design for a high power density ASTRON reactor, Lawrence Livermore National Laboratory, Livermore, CA, UCID-15731 (1970). Also issued in revised form as UCRL-72957 (1971) for submittal to Nucl. Fusion, but never published in that journal. Ralph Moir published this paper for Christofilos in J. Fusion Energy 8 (1989) 97.
- [27] A.E. Robson, in: B. Bruneli, G.G. Leotta (Eds.), The LINUS Concept, Unconventional Approach for Fusion, Plenum, New York, 1982.
- [28] R.W. Moir, Mirror Plasma Apparatus, U.S. Patent 4, 260, 455, April 7, 1981.
- [29] R.W. Moir, Rotating liquid blanket for a toroidal fusion reactor, Fusion Eng. Des. 5 (1987) 269.
- [30] R.W. Moir, Liquid first walls for magnetic fusion energy configurations, Nucl. Fusion 37 (1997) 557–566.
- [31] A.P. Fraas, The LLASCON—An Exploding Pellet Fusion Reactor, Oak Ridge National Laboratory, Oak Ridge, TN, TM-3231, 1971.
- [32] W.R. Meier, J. Am Maniscalco, Reactor Concepts for Laser Fusion, UCRL-79694, Lawrence Livermore National Laboratory, 1977.
- [33] M. Monsler, J. Maniscalco, J. Blink, J. Hovingh, W. Meier, P. Walker, Electric Power from Laser Fusion: The HYLIFE Concept, Proceeding of IECEC Conference, San Diego, CA, August 1978, p. 264.
- [34] J.A. Blink, et al., The High Yield Lithium Injection Fusion Energy (HYLIFE-I) Reactor, Lawrence Livermore National Laboratory, Livermore, CA, UCID-53559, 1985.
- [35] R.W. Moir, HYLIFE-II inertial confinement fusion reactor design, Fusion Technol. 19 (1991) 617.
- [36] M. Youssef, N. Morley, A. El-Azab, X-rays surface and volumetric heat deposition and tritium breeding issues in liquid-protected FW in high power density devices, to be published in Fusion Technol.
- [37] R. Woolley, Electromagnetically Restrained Lithium Blanket, IAEA Workshop on Innovative Approaches to Fusion Energy, Pleasanton, CA, 20–23 October, 1997.
- [38] C. Wong, et al., A helium-cooled blanket design of the low aspect ratio reactor, IAEA Technical Committee Meeting on Fusion Power Plant Design, Culham, UK, March, 1998, to be published in Fusion Eng. Des.
- [39] S. Malang, Limitations on Blanket Performance, to appear in Special Issue of Fusion Engineering and Design, Proceedings of SOFT-20, Marseilles, France, 1998.
- [40] D. Sze, Sn–Li, A Coolant/Breeder Material Developed for APEX/ALPS, presentation at the APEX meeting, 2–4 November, 1998 (full text available at <http://www.fusion.ucla.edu>).